JACS
JOURNAL OF THE AMERICAN CHEMICAL SOCIETY

COMMUNICATION

pubs.acs.org/JACS

Binary Heterogeneous Superlattices Assembled from Quantum Dots and Gold Nanoparticles with DNA

Dazhi Sun and Oleg Gang*

Center for Functional Nanomaterials, Brookhaven National Laboratory, Upton, New York 11973, United States

Supporting Information

ABSTRACT: Controllable assembly of three-dimensional (3D) superlattices composed of different types of nanoscale objects opens new opportunities for material fabrication. Herein we show the successful assembly of heterogeneous 3D structures from gold nanoparticles (AuNPs) and quantum dots (QDs) using DNA encoding. By applying synchrotron-based small-angle X-ray scattering, we found that AuNPs and QDs are positioned in a body-centered cubic lattice, while each particle type, AuNP and QD, is arranged in a simple-cubic manner. Our studies demonstrate a route for assembly of integrated heterogeneous 3D structures from different nano-objects by DNA-encoded interactions.

Incorporation of nucleic acids into nano-object design provides a powerful platform for the assembly of nanoscale objects in a highly controllable fashion. The ability to form well-defined three-dimensional (3D) ordered superstructures containing gold nanoparticles (AuNPs) using DNA as a programmable assembly agent has recently been demonstrated.[1−4] The rapidly developing theoretical understanding of assembly principles and involved interactions provide a base for future rational fabrication of nanomaterials by DNA means.[5−7] One of the most promising attributes of DNA-based assembly is an ability to direct interactions of different types of nanocomponents, encoded with DNA, into integrated systems, thus opening tremendous possibilities for material design. Although DNA-based heterogeneous assembly of different types of nanoparticles into clusters has been shown,[8−12] the formation of ordered 3D structures using DNA has been restricted to AuNPs and incorporations of organic species, molecular dyes, and viruses.[13,14] This is partially due to the difficulty in obtaining stable aqueous dispersions of inorganic nanoscale objects conjugated with DNA and the fine balance of interactions required for the formation of ordered structures.[1,3,15]

In this communication, we report the formation of a binary heterogeneous superlattice composed of quantum dot (QD)−AuNP 3D superlattices. Hybridization between complementary single-stranded DNA (ssDNA) correspondingly attached to the QDs and AuNPs readily induces system assembly. We have found that QD−AuNP assemblies form a body-centered cubic (BCC) lattice within which the AuNPs are positioned in a simple-cubic (SC) manner, as confirmed by in situ small-angle X-ray scattering (SAXS) measurements. Our studies have also provided a confirmation of the placement of complementary encoded particles within the unit cell of the BCC lattices. This question remained unresolved previously because the particles with the same inorganic core were used to carry different DNA encodings. This aspect is of high importance for understanding the phase behavior and future realization of programmable assembly.

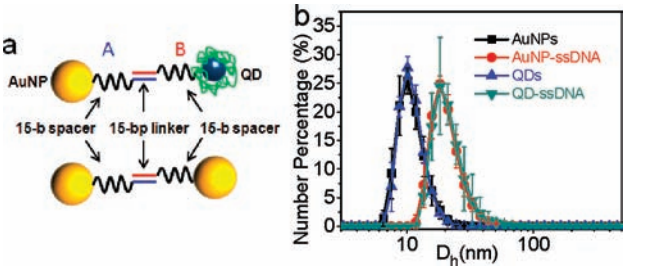

Figure 1. (a) Schematic illustration of the building blocks using in this study. The AuNPs were functionalized with thiolated ssDNA of type A, and the QDs were coated with a carboxyl-rich polymer shell (green) and conjugated with complementary amino-ssDNA of type B. (b) DLS data for bare AuNPs, bare QDs, AuNP−DNA conjugates, and QD−DNA conjugates.

We prepared the studied systems, shown in Figure 1a, by functionalization of 10 nm diameter AuNPs, as probed by dynamic light scattering (DLS) and electron microscopy [Figure 1b and Figure S1a in the Supporting Information (SI)], with 30-base (30-b) thiolated ssDNA of type A [A = 5′-TAC TTC CAA TCC AAT-$(T)_{15}$-C_3H_6-SH-3′, ∼60 DNA per AuNP]. This conjugation resulted in the formation of core−shell (AuNP−DNA) particles with a hydrodynamic diameter of ∼20 nm. CdSe−ZnS core−shell QDs (3−4 nm, Figure S1b) coated with a carboxyl-rich polymer shell, showing a hydrodynamic diameter of ∼10 nm (Figure 1b), were conjugated with 30-b amino-ssDNA of type B_{am} [B_{am} = 5′-ATT GGA TTG GAA GTA-$(T)_{15}$-NH_2-3′, ∼20 DNA per QD] through amine−carboxylic acid coupling (see the SI). The product QDs with polymer and DNA shells had a diameter of ∼20 nm, thus closely matching the size of the DNA-functionalized AuNPs. The observed similarity of the hydrodynamic diameters of the AuNPs and QDs, despite the 3-fold difference in DNA coverage, is due to the weak dependence of DNA thickness on grafted density[16] and the limits of DLS detection. For comparison experiments, the same AuNPs were also functionalized with 30-b thiolated ssDNA of type B_{th} [B_{th} = 5′-ATT GGA TTG GAA GTA-$(T)_{15}$-C_3H_6−SH-3′] to probe AuNP−AuNP assembly (see the SI and Figure 1a). The close match of the diameters of the DNA-coated AuNPs and QDs allowed for a direct and more quantitative comparison of AuNP−AuNP and

Received: January 4, 2011
Published: March 22, 2011

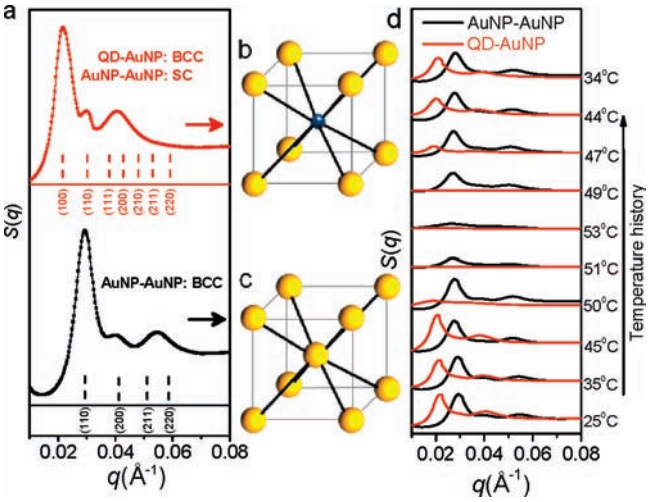

Figure 2. (a) SAXS patterns of AuNP−AuNP and QD−AuNP assemblies. (b) Cartoon of the crystal unit for the QD−AuNP assembly. (c) Cartoon of the crystal unit for the AuNP−AuNP assembly. (d) Temperature-dependent SAXS patterns for the AuNP−AuNP assembly (black) and the QD−AuNP assembly (red).

QD−AuNP systems. Both type-A and type-B (either B_{am} or B_{th}) DNA strands contained 15-b poly(T) segments as a spacer and a 15-base outer complementary segment, allowing the nanoparticles to assemble through the formation of 15 base pair (bp) duplexes. To form QD−AuNP and AuNP−AuNP assemblies, we mixed equal amounts of type-A and type-B nanoparticles in 50 mM borate buffer (pH = 7.4, [NaCl] = 0.1 M), incubated the mixture at 60 °C for 10 min, and allowed it to cool to room temperature overnight.

We applied synchrotron-based SAXS (performed using beamline X9 at the National Synchrotron Light Source) to investigate the structure and temperature evolution of the obtained assemblies in situ. Figure 2a illustrates the structure factors $S(q)$ as a function of scattering vector q for both QD−AuNP and AuNP−AuNP assemblies. $S(q)$ values were obtained from azimuthally integrated 2D SAXS patterns after normalization by a form factor, measured from the solution containing the equimolar mixture of free particles. The binary AuNP−AuNP assembly exhibited a diffraction pattern matching that of a BCC lattice (Figure 2c), as previously reported. The ratio of the positions of the first-order (q_1 = 0.029 Å^{-1}) and second-order (q_2 = 0.041 Å^{-1}) diffraction peaks was 1:$\sqrt{2}$, and these peaks are attributed to diffraction from the (110) and (200) planes, respectively.[1] The nearest-neighbor distance d_{nn} of ∼26 nm corresponds to the center-to-center (16 nm surface-to-surface) distance between AuNPs located in the center to corner of the BCC lattice, which is in agreement with our previous results.[1] In contrast, the QD−AuNP system, despite the similar sizes of DNA-coated QDs and AuNPs and the use of the same DNA motifs, showed a different diffraction pattern, with the first peak being significantly shifted to lower q (0.021 Å^{-1}). The structure can be understood by taking into account the 30−50-fold reduction in the number of electrons in a QD relative to an AuNP, which results in a relatively low scattering cross-section for the QDs. This relatively low contrast of QDs in our SAXS measurements masks the presence of QDs, which are expected to be located in the centers of the BCC units. In this case, the main contribution to the scattering is provided by AuNPs in the corners of BCC. That corresponds to the arrangement of AuNPs in a SC lattice (Figure 2b). Indeed, we found that the measured SAXS profile agrees surprisingly well with the SC lattice, as shown in Figure 2a. The q_1/q_2 ratio in the diffraction pattern of the QD−AuNP assembly is equal to 1:$\sqrt{2}$, which corresponds to the (100) and (110) planes of the SC lattice, respectively. For this SC arrangement of the AuNPs, we obtain the distance from the cube center, where QD is located, to AuNP at the cube corner. That allows estimating a nearest-neighbor, QD to AuNP, distance d_{nn}= 25 nm. The estimation is in close agreement with our measurements for the AuNP−AuNP assembly for d_{nn} is about 26 nm. In a control experiment, we studied a QD−QD binary assembly using type-A and type-B ssDNA. The same SAXS setup did not show any noticeable diffraction pattern (see Figure S2), confirming the low scattering intensity of the QDs. Thus, the size similarity of AuNP and QD shelled particles and their large difference in scattering intensity allowed for unambiguous determination of the structure of the heterogeneous assembly, in which the QDs and AuNPs form a BCC lattice in which the AuNPs are arranged in an SC fashion.

The homogeneous (AuNP−AuNP) and heterogeneous (QD−AuNP) systems not only exhibited analogous structures but also demonstrated a similar kinetic pathway. We observed that the crystallinity of the assemblies was improved after annealing in comparison with the assemblies formed at room temperature (see Figure S3), which agrees with our previous reports.[1,3] At the same time, the homogeneous and heterogeneous systems exhibited essential differences. For example, we performed experiments for the QD−AuNP assemblies by using longer ssDNA strands (see Figure S4a), with motifs resulting in crystalline organizations.[1] However, this motif in our heterogeneous system showed only a weak order that did not improve after annealing (see Figure S4b), which is in contrast to the behavior of the analogous homogeneous systems. We attribute this to (i) unequal DNA coverage on the AuNPs and QDs (∼20 per QD and ∼60 per AuNP) and (ii) the polymer layer on the QDs. Both factors contribute to additional repulsions and result in modified interparticle interactions. Such unequal DNA coverage on the particles might in future designs allow for a tailored modulation of interactions due to the confinement of unhybridized chains. Interestingly, the binary QD−AuNP systems with QDs containing lower numbers of DNA strands (∼9 per QD) formed only small submicrometer clusters that did not exhibit any noticeable SAXS pattern (see Figure S5). The above experimental results demonstrate that the DNA coverage on the QDs has a profound effect on the phase behavior of QD−AuNP assemblies and that in order to obtain ordered QD−AuNP assemblies, high DNA coverage on the nanoscale building blocks is needed. Additionally, the QD−AuNP assembly exhibits a looser packing density than the AuNP−AuNP assembly, as observed by the scanning electron microscopy (see Figure S6), which is due to the significantly low contrast of QDs compared to AuNPs within the assembled aggregates.

Temperature-dependent synchrotron-based SAXS was utilized to monitor the thermal behavior of the QD−AuNP assemblies and superlattice disassembly due to duplex melting. Figure 2d illustrates the scattering patterns of AuNP−AuNP and QD−AuNP assemblies during one thermal cycle of heating and cooling. The QD−AuNP assembly showed a slight broadening of the melting transition accompanied by a 3° lower melting temperature relative to the analogous AuNP−AuNP system. This observation is consistent with lower DNA coverage on the QDs, resulting in a smaller local density of duplexes, and was also reported for the AuNP systems.[17] The assembly/disassembly process was fully reversible, as confirmed by the structure

dx.doi.org/10.1021/ja111542t |J. Am. Chem. Soc. 2011, 133, 5252–5254

recovery upon subsequent cooling after melting (Figure 2d). Moreover, the diffraction pattern of the QD−AuNP assembly shifted to lower q values upon heating (d_{nn} changed from ~25 to ~28 nm) and moved back toward its original position upon cooling. This phenomenon is the result of a thermally induced lattice change, which is also consistent with the AuNP−AuNP assembly.

In summary, we have demonstrated the formation of a binary heterogeneous QD−AuNP superlattice via DNA-mediated programmable assembly. Our experiments revealed that AuNPs form a SC lattice in the heterogeneous superlattice. By comparing the QD−AuNP and AuNP−AuNP systems built from the similar sized particles and DNA, we concluded that the superlattice exhibited a BCC structure in which the QDs and AuNPs were placed in well-defined positions, with AuNPs positioned in the corners of the BCC lattice, thus forming an SC arrangement, and the QDs located at the cube centers. Our results allowed the differentiation of the positions of particles with different encodings and hence provided an experimental evidence regarding the location of particles of different types within the unit cell of the BCC lattice. Our studies have also demonstrated an approach for the construction and characterization of heterogeneous assembles where particles of different types are positioned in 3D by biomolecular linkers. The functional properties of such heterogeneous nanomaterials are waiting to be explored. For instance, the described 3D system containing fluorescent (QD) and plasmonic (AuNP) might demonstrate optical effects governed by collective contributions of particles in such lattices.

■ ASSOCIATED CONTENT

Supporting Information. Additional experimental details and TEM, DLS, and SAXS results. This material is available free of charge via the Internet at http://pubs.acs.org.

■ AUTHOR INFORMATION

Corresponding Author
ogang@bnl.gov

■ ACKNOWLEDGMENT

Research was carried at the Center for Functional Nanomaterials, Brookhaven National Laboratory, which is supported by the U.S. Department of Energy, Office of Basic Energy Sciences, under Contract No. DE-AC02-98CH10886. Use of the National Synchrotron Light Source, Brookhaven National Laboratory, was supported by the U.S. Department of Energy, Office of Science, Office of Basic Energy Sciences, under Contract No. DE-AC02-98CH10886. We also thank C. Chi for nanoparticle synthesis, D. Nykypanchuk for help with SAXS measurements, and E. Stach for high-resolution TEM imaging of QDs.

■ REFERENCES

(1) Nykypanchuk, D.; Maye, M. M.; van der Lelie, D.; Gang, O. *Nature* **2008**, *451*, 549.
(2) Park, S. Y.; Lytton-Jean, A. K. R.; Lee, B.; Weigand, S.; Schatz, G. C.; Mirkin, C. A. *Nature* **2008**, *451*, 553.
(3) Xiong, H. M.; van der Lelie, D.; Gang, O. *J. Am. Chem. Soc.* **2008**, *130*, 2442.
(4) Macfarlane, R. J.; Jones, M. R.; Senesi, A. J.; Young, K. L.; Lee, B.; Wu, J. S.; Mirkin, C. A. *Angew. Chem., Int. Ed.* **2010**, *49*, 4589.
(5) Tkachenko, A. V. *Phys. Rev. Lett.* **2002**, *89*, No. 148303.
(6) Scarlett, R. T.; Crocker, J. C.; Sinno, T. *J. Chem. Phys.* **2010**, *132*, No. 234705.
(7) Hsu, C. W.; Sciortino, F.; Starr, F. W. *Phys. Rev. Lett.* **2010**, *105*, No. 055502.
(8) Mitchell, G. P.; Mirkin, C. A.; Letsinger, R. L. *J. Am. Chem. Soc.* **1999**, *121*, 8122.
(9) Maye, M. M.; Nykypanchuk, D.; Cuisinier, M.; van der Lelie, D.; Gang, O. *Nat. Mater.* **2009**, *8*, 388.
(10) Mastroianni, A. J.; Claridge, S. A.; Alivisatos, A. P. *J. Am. Chem. Soc.* **2009**, *131*, 8455.
(11) Maye, M. M.; Gang, O.; Cotlet, M. *Chem. Commun.* **2010**, *46*, 6111.
(12) Wang, Q. B.; Wang, H. N.; Lin, C. X.; Sharma, J.; Zou, S. L.; Liu, Y. *Chem. Commun.* **2010**, *46*, 240.
(13) Xiong, H. M.; Sfeir, M. Y.; Gang, O. *Nano Lett.* **2010**, *10*, 4456.
(14) Cigler, P.; Lytton-Jean, A. K. R.; Anderson, D. G.; Finn, M. G.; Park, S. Y. *Nat. Mater.* **2010**, *9*, 918.
(15) Xiong, H.; van der Lelie, D.; Gang, O. *Phys. Rev. Lett.* **2009**, *102*, No. 015504.
(16) Dan, N.; Tirrel, M. *Macromolecules* **1992**, *25*, 2890.
(17) Jin, R. C.; Wu, G. S.; Li, Z.; Mirkin, C. A.; Schatz, G. C. *J. Am. Chem. Soc.* **2003**, *125*, 1643.